J Mater Sci: Mater Electron (2013) 24:1037–1044
DOI 10.1007/s10854-012-0874-7

Interfacial reaction of Sn–2.0Ag–2.5Zn solder on Cu and Ni–W substrates

Yucheng Liu · Anmin Hu · Tingbi Luo · Ming Li

Received: 4 June 2012 / Accepted: 13 August 2012 / Published online: 28 August 2012
© Springer Science+Business Media, LLC 2012

Abstract The interfacial reactions of Sn–2.0Ag–2.5Zn solder on Cu and Ni–W substrates after soldering and subsequent aging have been investigated in this study. Ni–W alloy layers with tungsten content of 3.0 and 10.0 at.% were electrodeposited on copper substrate. The interfacial micrographs of solder joints prepared at 250 °C for 15 s and aged at 150 °C for 24, 96 and 216 h are shown. Double-layer IMC composed of Cu_5Zn_8 and Ag_3Sn was observed at the interface of Sn–2Ag–2.5Zn and Cu couple, which was compact and acted as a barrier layer to confine the further growth of Cu–Sn IMC. On Ni–W barrier layer, a thin Ni_3Sn_4 film appeared between the solder and Ni–W layer, whose thickness decreases with the increase of W content. During the aging process, a thin layer of the Ni–-W substrate transforms into an amorphous bright layer, and the thickness of amorphous layer increased as aging time extended. Referring to the elemental line-distribution and the thickness of different layers at the interface, the formation of the bright layer is caused by the fast diffusion of Sn into Ni–W layer.

1 Introduction

Sn-based Pb-free solders e.g. Sn–Ag, Sn–Zn have been gradually become dominating bumping materials in reflow technology. To reduce the cost of Sn–Ag solder which has been accepted as the most promising substitute for Sn–Pb, low Ag content Sn–Ag has been a focus of Pb-free solders research, including Sn–Ag–Cu and Sn–Ag–Zn solders [1–5]. Sn–Ag–Zn solder has been proven that it possesses much superiority, such as strength and the inhibition of intermetallic compounds (IMC) growth inside solder [6], and at the solder joint interface [7]. In our previous research, we have developed one type of Sn–Ag–Zn solder with 2.0 wt% Ag and 2.5 wt% Zn content (Sn–2Ag–2.5Zn), which owns good performance in strength [8].

The integrity of interface between solder and substrate is of vital importance in assuring the reliability of solder joints in electronic products, and the morphology and growth behavior of IMC at the interface plays a crucial role. The IMC is always brittle, and a thick and uneven IMC layer will damage the reliability of the bonding. When conventional Sn–Ag solder is used to join a bare copper substrate, it reacts quickly at the interface, forming a thick and irregular IMC layer(s) which impacts the reliability [9, 10]. Nickel is usually used as the barrier layer material in electronic industry, because of its relatively lower reaction rates with solders and copper [11, 12]. Thus it can limit the reaction at the interface. However, it has been proved that the Nickel film is consumed rapidly during high temperature aging. The addition of P, V and W to the Nickel film has attracted a great deal of attention in recent years, especially the Ni–W alloy film [13–15]. The low diffusion coefficient of W atoms in Ni and their segregation to grain boundaries make the alloy film more stable. There are some investigations about the Sn–Ag/Ni–W interfacial reactions [14], but reports on ternary low Ag content solder are rare.

In this study, the growth behavior of interfacial IMC between Sn–2Ag–2.5Zn and copper substrate or Ni–W barrier film (Ni-3 at.% W and Ni-10 at.% W) has been investigated through the examination of the morphologies at different aging times (24, 96, 216 h) at 150 °C. The effect of W content in the barrier film on the IMC growth

Y. Liu · A. Hu (✉) · T. Luo · M. Li
State Key Lab of Metal Matrix Composites,
Shanghai Jiao Tong University, Shanghai 200240, China
e-mail: huanmin@sjtu.edu.cn

behavior at the interface after different aging times has also been investigated.

2 Experimental procedures

For this study, Sn–Ag–Zn with 2.0 wt% Ag and 2.5 wt% Zn content (Sn–2Ag–2.5Zn) Pb-free solder was prepared from ingots of pure Sn, Ag and Zn (with a purity of 99.99 %). The process of melting was carried out in a corundum crucible; the surface was covered with KCl–LiCl salt in order to prevent evaporation and oxidation of the elements. Then the crucible was placed in a box-type resistance furnace at 600 °C for 30 min to promote melting. Alloy was stirred every 5 min during the heating process for adequate homogenization. The solder was cut into pieces weighing 0.1 g, and melted to make solder balls in liquid colophony.

Copper sheet of dimension 0.5 mm × 20 mm × 50 mm was used as the substrate. Ni–W alloy films were prepared on copper substrate by electrodeposition. Before soldering or electrodepositing, the Cu substrate was cleaned with detergent and dipped in 20 vol.% H_2SO_4 to clean the surface and get rid of the oxide layer. It was rinsed with distilled water followed by drying with acetone. Electrodeposition of Ni–W alloys films was carried out in an ammonia citrate baths maintained at 80 °C. Deposition current density was 10 mA/cm^2 and Ni alloy films were deposited to a thickness about 2.0 μm.

The solder ball was soldered on the substrate at 250 °C using 30 wt% colophony ethanol solution as flux. The soldering process lasted for 15 s, it cooled in the air environment. The samples were placed in the furnace and aged at 150 °C for 24, 96, and 216 h. Samples were prepared for cross sectional examination by standard metallographic technique. Scanning electron microscopy with the backscattering electron image (BEI) was used for microstructural examination. The average thickness of the interfacial IMC layer was measured by dividing the area covered by the layer by its length with Adobe Photoshop CS4. For each experimental condition, the average thickness was calculated from at least four micrographs taken at randomly selected position on the cross sectional samples. The elemental analysis of different phases and element line distribution were carried out by energy dispersive X-ray spectroscopy (EDX).

3 Results and discussion

3.1 Microstructure evolution of solder/Cu couple

The BEI micrographs of the interface between Sn–2Ag–2.5Zn and Cu substrate after soldering before aging is shown in Fig. 1. The figure reveals that the thin IMC thickness is about 1 μm growing into the solder. Elemental ratio determined by EDX is presented in Table 1. The atoms of Cu, Ag, Zn and Sn have gathered at the interface to generate IMC. The composition of the area is complex and the IMC cannot be identified. Figure 2 shows the interfacial morphologies after aging at 150 °C for 24 h. The thickness of the IMC increases evidently. Two reaction layers formed.

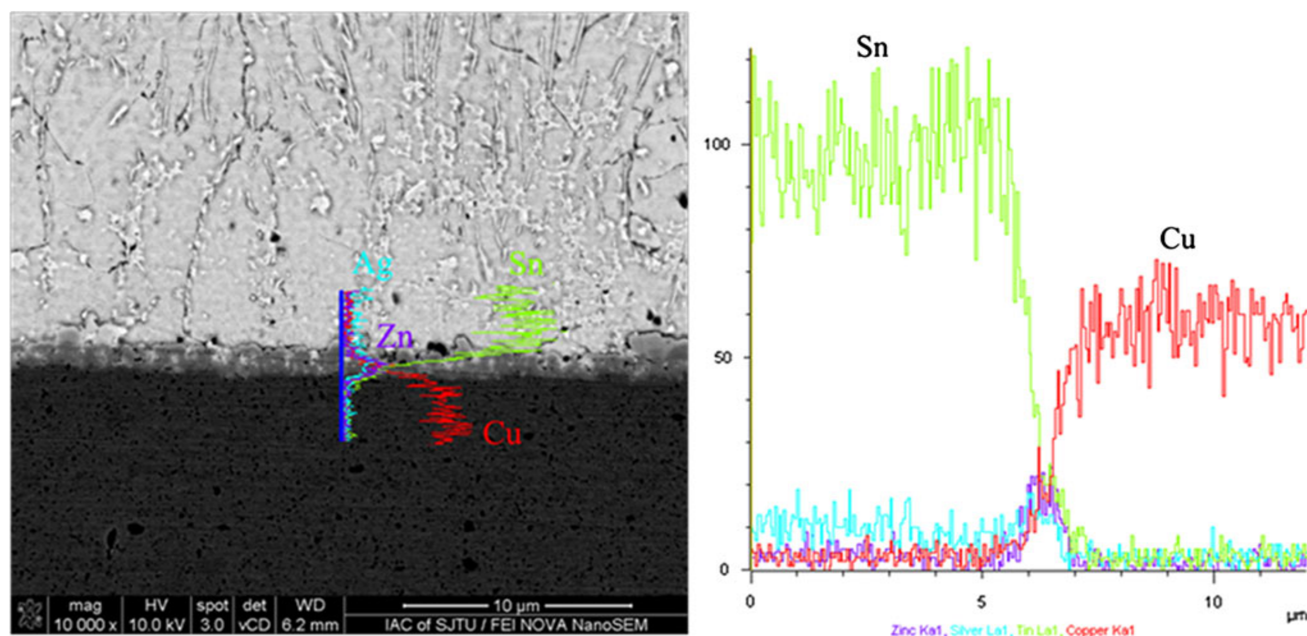

Fig. 1 BEI micrograph and EDS line analysis of Sn–2Ag–2.5Zn/Cu interface after soldering at 250 °C for 15 s

Table 1 Elemental ratio of IMC layer after soldering for 15 s

Element	Atomic (%)
Cu	11.50
Zn	62.66
Ag	23.37
Sn	2.46

The elemental ratio of the layer adjacent to copper substrate is examined with EDX, and according to the atomic ratio and the relevant references [12, 16], it is presumed that the phase is Cu_5Zn_8. The elemental composition of the IMC layer adjacent to the solder detected by EDX is consistent with Ag_3Sn. To learn more about the structure and the formation of the two-layer IMC at the interface, we delineated the element distribution of the interfacial area with EDX. The result is shown in Figs. 1 and 2 simultaneously. The elements concentrate at the interface after soldering to form a complex IMC layer, and the element ratio is given in Table 1. After aging for 24 h, the structure and element distribution of the IMC layers becomes clear. Copper diffuses towards to the solder, and zinc concentrated at the area adjacent to the copper substrate to form Cu_5Zn_8, whereas silver and tin gathered next to the Cu–Zn layer to form Ag_3Sn.

Figure 3a, b shows the BEI images of the morphology of the interface after aging for 96 and 216 h. The growth of the IMC carried out gradually as the aging time extends. Not only is the thickness increasing, but also the shape of the IMC film is changing and the two layers structure is more apparent. The area of Ag_3Sn layer covering on the interface is expanding, whereas its thickness keeps stable. The thickness of IMC increased slowly with the aging time and maintained under 5 μm showing, which indicate the promising reliability of the interface.

According to growth kinetics principles and referring to some other related research results [16], the IMC growth behavior can be explained as follows. Immediately after soldering, owing to the high activation energy and the kinetic of forming IMC, element atoms approached the interface and a thin and complex IMC layer forms. During the aging process, Zn is able to react with Cu and Ag to form IMC, but because of higher growth kinetics, Zn predominantly reacts with Cu to form Cu–Zn IMC (Cu_5Zn_8), and Ag may compete with Cu for Zn to the form of Ag–Zn IMC (mostly $AgZn_3$) next to the Cu–Zn layer. As most of the Zn reacts with Cu and the Zn content of the solder is low, the remaining amount of Zn atoms is small and the formation of $AgZn_3$ is too rare to be detected at the interface. With the consumption of Zn, the relative proportion of Sn and Ag rises up, and the continuous layer of Ag_3Sn is generated next to the Cu_5Zn_8 layer as the aging time extends. As these two continuous layers of IMC form at the interface, they act as barrier layers to prevent the excessive growth of Cu–Sn and Cu–Zn IMC, which limits the thickness of IMC under 5 μm after aging for 216 h to ensure the reliability of the bonding.

3.2 Microstructure evolution of solder/electroplated Ni–W substrates

Two different W content Ni–W alloy barrier layers (Ni-3 at.% W and Ni-10 at.% W) were studied in the experiment. In order to protect the substrate from oxidation, the

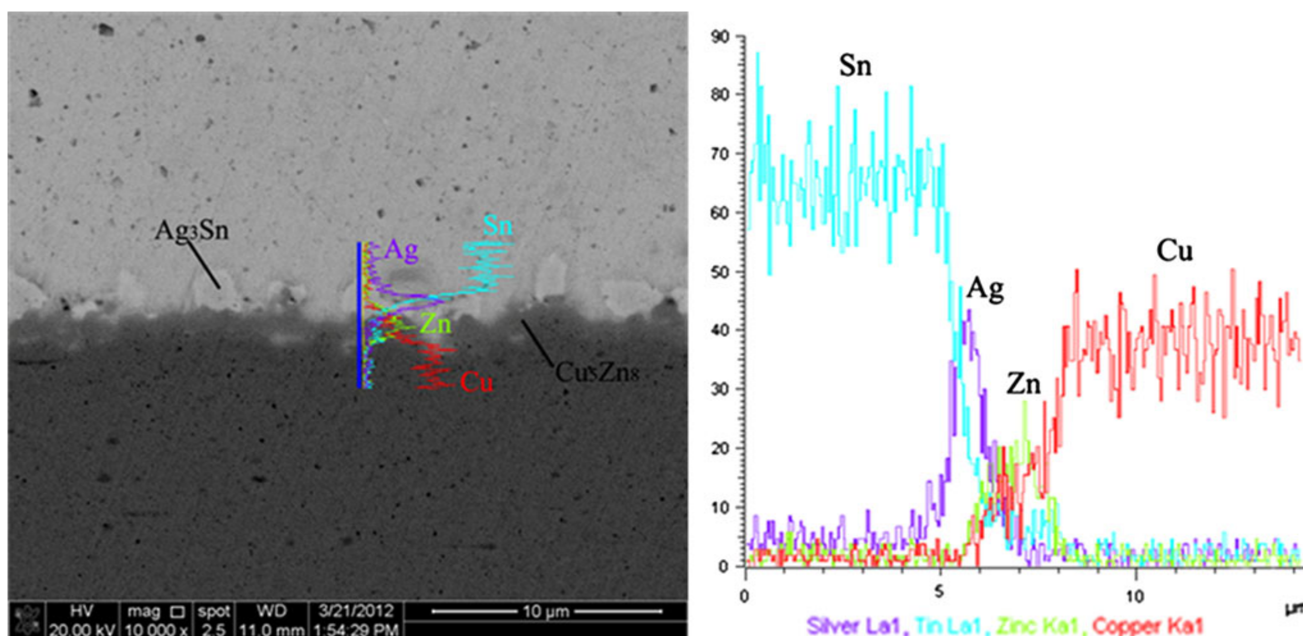

Fig. 2 BEI micrograph and EDS line analysis of Sn–2Ag–2.5Zn/Cu interface after aging at 150 °C for 24 h

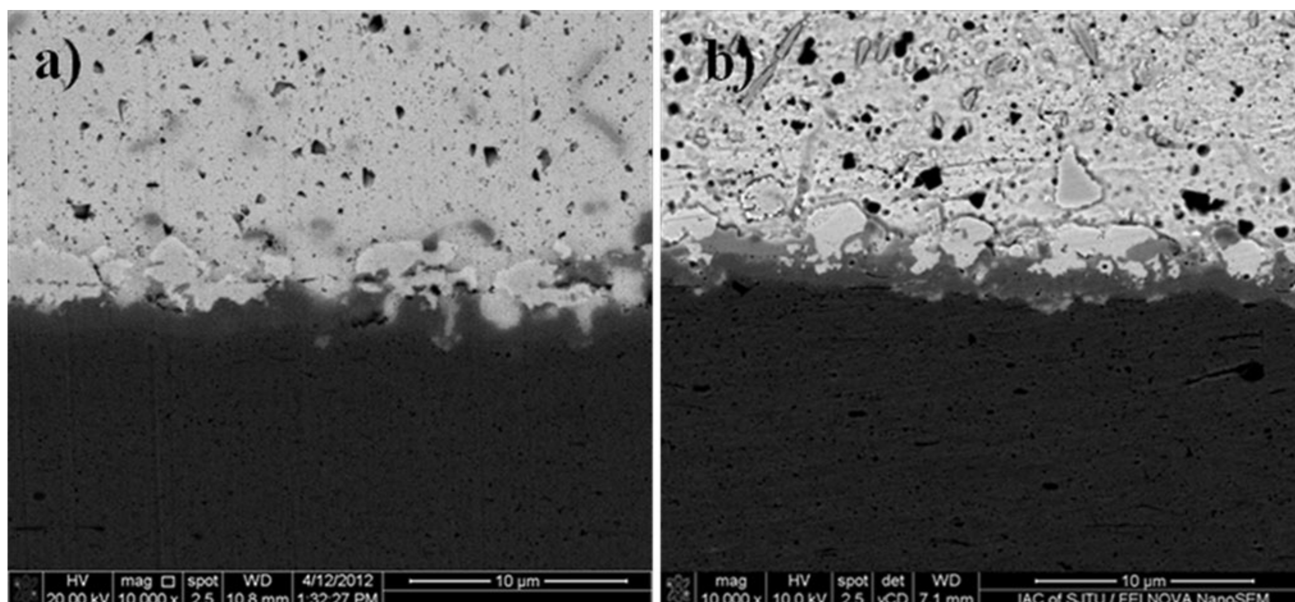

Fig. 3 BEI micrograph of Sn–2Ag–2.5Zn/Cu interface after aging at 150 °C for different time: **a** 96 h, **b** 216 h

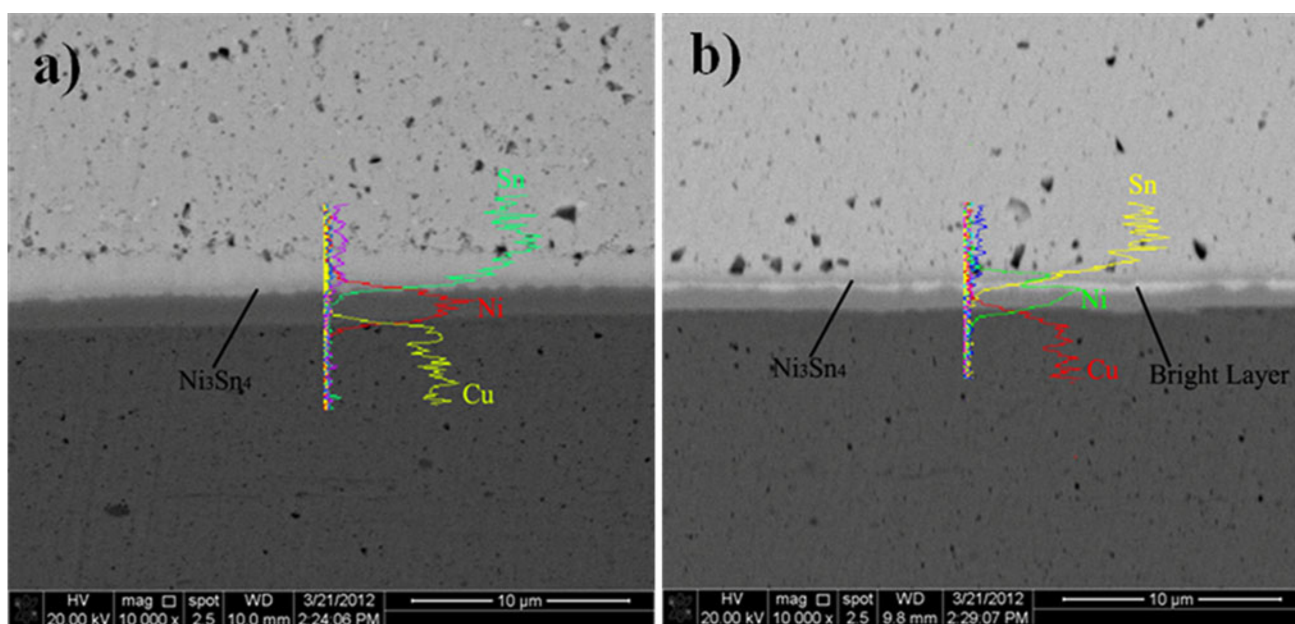

Fig. 4 BEI micrograph and EDS line analysis of interface after soldering at 250 °C for 15 s for different barrier layers: **a** Ni-3 at.% W, **b** Ni-10 at.% W

soldering was carried out immediately after electroplating. Figure 4a, b show the cross-section micrograph of the Sn–2Ag–2.5Zn/Ni–W couple soldering at 250 °C for 15 s respectively. The interfacial microstructure is different from that in the Sn–2Ag–2.5Zn/Cu couple. There is no massive irregular IMC at the interface, but thin and compact IMC layers covering on the barrier layers which thickness is only 0.5–0.8 μm. The composition of the IMC layer was analyzed by EDX, and it can be identified as Ni_3Sn_4. There appears a bright layer between the Ni_3Sn_4 and Ni-10 % W film, which has been reported in earlier study as an amorphous film formed at the interface between Sn and Ni–W [14]. Element line-distribution analyses at the interfacial area are also shown in Fig. 4a, b. The Ni–W barrier film is about 2 μm, and separates the solder and the copper substrate. The atoms from both solder and copper sides have not crossed the barrier film to form X-Cu IMC. There is a decreasing trend of the nickel content profile at

Table 2 Elemental ratio of bright layer on different Ni–W barrier layer

Barrier film	Composition of bright layer, at.%		
	Ni	W	Sn
Ni-3 at.% W	27.53	20.41	52.06
Ni-10 at.% W	16.41	32.69	50.90

the bright layer between Ni_3Sn_4 and Ni-10 % W. Table 2 shows the elemental ratio of the bright layer. Referring to the element line-distribution and point scan result, it reveals that Sn atoms and Ni atoms diffuse into each other, while W atoms stay in the barrier layer, the content ratio of W on nickel rises up, becoming much higher than the original ratio of the barrier film.

Solid state amorphization in thin layer systems has been investigated [17–19]. It has been considered that solid state amorphization between two components thin films configuration can occur under the following circumstances: (1) the two components possess a large negative heat of mixing in the amorphous state, (2) one component has anomalously high diffusion coefficient compared with the other, and (3) reaction occurs at a temperature low enough to suppress the nucleation/growth of thermodynamically preferred crystalline phases. In the present case, condition (2) and (3) are believed to have been satisfied. Other research shows that if W content is more than 25 at.% in Ni, it transforms into an amorphous film, which is correspondent to the present result [14]. The amorphous layer is believed to be an effective barrier owning to its low diffusivity.

Figure 5 is the micrograph of the interface after aging for 24 h, showing that the thickness of the IMC layer didn't increase significantly compared with on copper substrates. The thickness of the bright layer in Fig. 5b is increasing, through the consumption of the barrier layer. Referring to element line-distributions shown in Fig. 5a, b, there is still no sign of accumulation of other element atoms adjacent to the barrier layer.

The interfacial micrographs of different Ni–W substrates after aging 96 h is shown in Fig. 6a, b. In Fig. 6a, bright layer is observed to have appeared between the Ni_3Sn_4 and Ni-3 % W, with elemental ratio shown in Table 2. EDX line scan on the element distribution is shown in Fig. 6a simultaneously. This reveals that the principle of the generation of the bright layer is similar to Ni-10 % W. With the penetration of the Sn and Ni into each other, the increase of the W content ratio on Ni leads to the formation of the amorphous film in the bright layer.

Figure 7a, b show the micromorphology and element line-scan results after 216 h aging process. As the aging time extends to 216 h, the thickness of the IMC increases slowly whereas the bright layer keeps growing thicker and consuming the barrier film with the aging process, which is correspondent to the continuous diffusion of Sn and Ni atoms into each other during the aging process. The other elements (Ag and Zn) are still isolated on the solder side, with no segregation phenomena at the interface in contrast to the copper substrate.

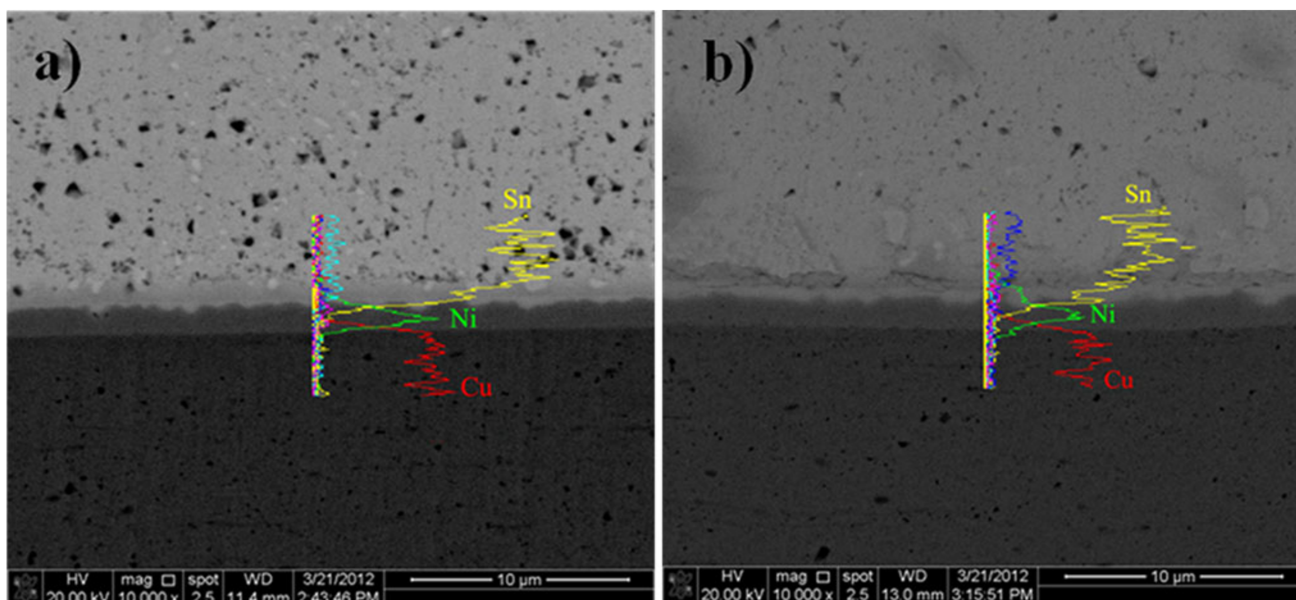

Fig. 5 BEI micrograph and EDS line analysis of interface after aging at 250 °C for 24 h for different barrier layers: **a** Ni-3 at.% W, **b** Ni-10 at.% W

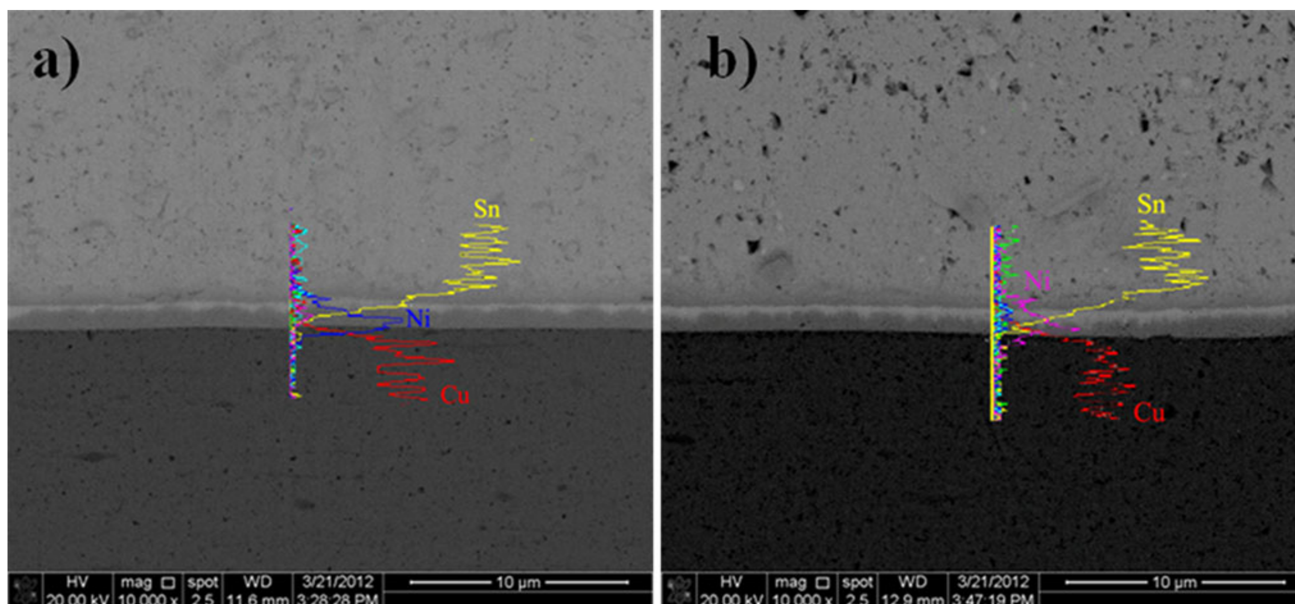

Fig. 6 BEI micrograph and EDS line analysis of interface after aging at 250 °C for 96 h for different barrier layers: **a** Ni-3 at.% W, **b** Ni-10 at.% W

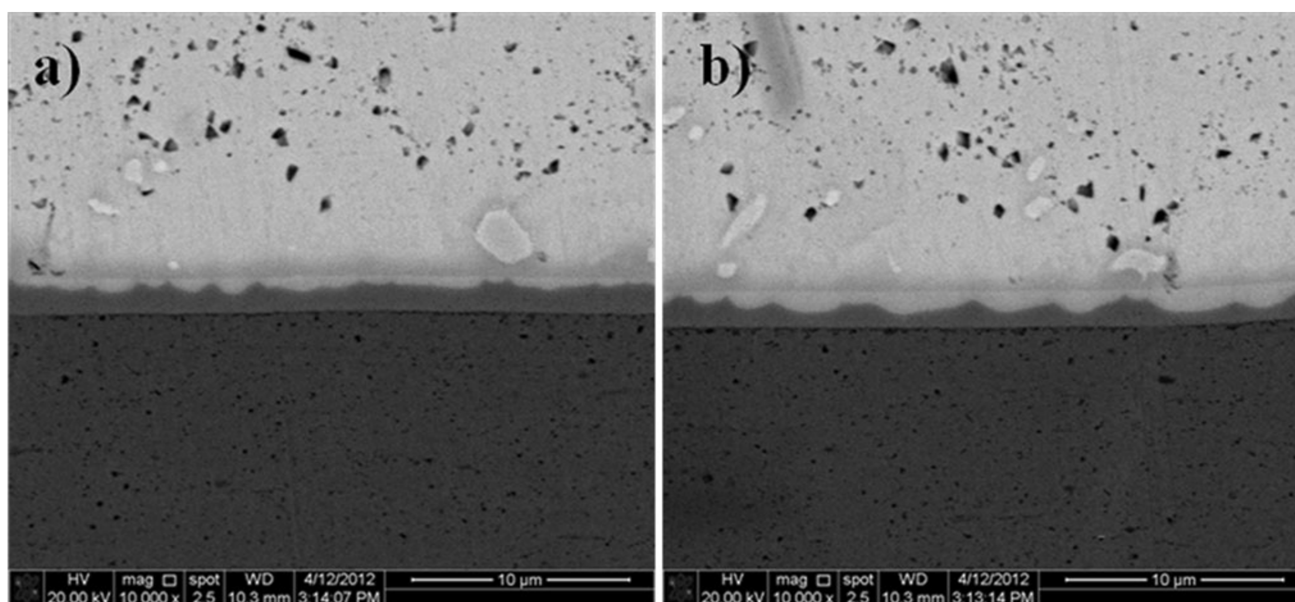

Fig. 7 BEI micrograph of interface after aging at 250 °C for 96 h for different barrier layers: **a** Ni-3 at.% W, **b** Ni-10 at.% W

The average thickness of Ni_3Sn_4, bright layer and remaining barrier layer of Ni-3 % W and Ni-10 % W after different aging time are shown in Fig. 8. The data was calculated from at least three micrographs taken randomly selected position at the interface. It's revealed that both in the cases of Ni-3 % W and Ni-10 % W, right after aging process, the thickness of Ni3Sn4 rapidly increased, and with the aging time extending, the thickness remained around a stable value, showing no appearance of substantially thickening. It reveals that the diffusion Ni atom into solder is weak, and the barrier layer itself is stable. A steady decrease of Ni_3Sn_4 thickness is observed with the increase in W content in barrier layer-the thickness of Ni_3Sn_4 of Ni-10 % W is about 0.5–1 μm less than that of Ni-3 % W. After the formation of bright layer, the thickness of Ni_3Sn_4 increases slowly or keeps stable. The thickness of Ni-10 % W is about 0.5 μm thicker than that of Ni-3 % W, which might be the reason for the decrease of Ni-$_3Sn_4$ with the increase of the W content. The bright layer of Ni-3 % W appeared after aging for 96 h, while for

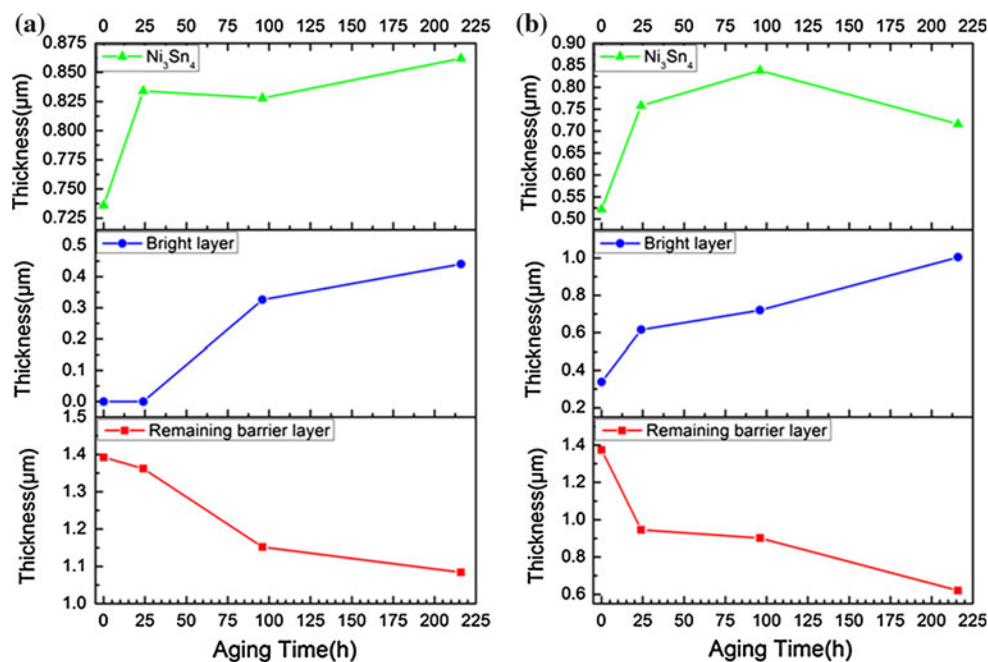

Fig. 8 Variation of the thickness of Ni3Sn4 IMC, bright layer, and remaining Ni–W layer as a function of aging time of different Ni–W layer: **a** Ni-3 at.% W, **b** Ni-10 at.% W

Ni-10 % W it formed right after the soldering process, which indicates the W content of Ni–W layer is a critical factor of the appearance of bright layer. With the appearance of the bright layers, the thickness of remaining barrier layer came down, and the reduction of the barrier layer simply equals the addition of the bright layer. It means that the Ni and W atoms rarely diffuse into the solder and the consumption of the barrier layer is mainly caused by the diffusion of Sn atom into the barrier layer, transforming the barrier layer into bright layer, which is confirmed by the result of elemental line scans.

4 Conclusions

In this study, interfacial reactions between Sn–2.0Ag–2.5Zn solder and different substrates (Cu, Ni-3 at.% W, Ni-10 at.% W) were studied. On the copper substrate, Sn–2Ag–2.5Zn reacted with copper to form double-layer IMC: (1) due to kinetics, compact Cu_5Zn_8 formed next to the copper substrate; (2) the remaining Sn and Ag reacted to form Ag_3Sn next to the Cu_5Zn_8 layer. The double-layer IMC prevent the atom from further diffusing, to confine the thickness of IMC under 5 μm after aging for 216 h at 150 °C. On the Ni–W barrier layer, only Ni_3Sn_4 was found as the main IMC between solder and substrate, and its thickness decreases with the increase of W content in the Ni–W layer. The other alloy elements in the solder were not observed to gather at the interface to form IMC, As the aging time extended, Sn diffused into barrier layer faster than Ni into solder and an amorphous layer appeared between Ni3Sn4 and Ni–W layers. The appearance of this amorphous layer is more apparent on the Ni-10 % W substrate. If the aging time extends, Sn might diffuse across the Ni–W layer into the copper, so the long term reliability of the Sn–2Ag–2.5Zn solder on different substrates requires further investigation.

Acknowledgments This work was sponsored by International Science and Technology Cooperation of China (No. 2011ZX02702) and National Natural Science Foundation of China (No. 61176097).

References

1. H.T. Lee, Y.H. Lee, Mater. Sci. Eng. A **419**, 172–180 (2006)
2. C.M. Chuang, P.C. Shih, K.L. Lin, J. Electron. Mater. **33**, 1–6 (2004)
3. I. Shohji, T. Yoshida, T. Takahashi, S. Hioki, Mater. Sci. Eng. A **366**, 50–55 (2004)
4. X. Zhang, H. Wang, Y. Shi, J. Mater. Sci. Mater. Electron. **15**, 511–517 (2004)
5. M. El-Bahay, M. El Mossalamy, M. Mahdy, A. Bahgat, J. Mater. Sci. Mater. Electron. **15**, 519–526 (2004)
6. J. Shen, S. Lai, Y. Liu, H. Gao, J. Wei, J. Mater. Sci. Mater. Electron. **19**, 275–280 (2008)
7. F.J. Wang, F. Gao, X. Ma, Y.Y. Qian, J. Electron. Mater. **35**, 1818–1824 (2006)
8. T. Luo, X. Chen, J. Hu, A. Hu, M. Li, IEEE, 399–404 (2010)
9. C. Hwang, K.S. Kim, K. Suganuma, J. Electron. Mater. **32**, 1249–1256 (2003)
10. M.S. Suh, C.J. Park, H.S. Kwon, Mater. Chem. Phys. **110**, 95–99 (2008)
11. K.S. Kim, J.M. Yang, C.H. Yu, I.O. Jung, H.H. Kim, **379**, 314–318 (2004)
12. C.Y. Lee, J.W. Yoon, Y.J. Kim, S.B. Jung, Microelectron. Eng. **82**, 561–568 (2005)
13. C.C. Chen, S.W. Chen, J. Electron. Mater. **35**, 1701–1707 (2006)
14. A.S.M.A. Haseeb, C. Chew, M.R. Johan, J. Mater. Sci. Mater. Electron. **22**, 1372–1377 (2011)

15. H. Kotadia, O. Mokhtari, M. Bottrill, M. Clode, M. Green, S. Mannan, J. Electron. Mater. **39**, 2720–2731 (2010)
16. K.L. Lin, C.L. Shih, J. Electron. Mater. **32**, 95–100 (2003)
17. R. Benedictus, C. Træholt, A. Böttger, E. Mittemeijer, Thin Solid Films **345**, 319–329 (1999)
18. B. Liu, W. Lai, Z. Zhang, Adv. Phys. **50**, 367–429 (2001)
19. R. Schwarz, W. Johnson, Phys. Rev. Lett. **51**, 415–418 (1983)